How to cite: *Angew. Chem. Int. Ed.* **2024**, *63*, e202409115
doi.org/10.1002/anie.202409115

Carbene Chemistry

A [2.2]Isoindolinophanyl-Based Carbene (iPC) Ligand: Synthesis, Electronic and Photophysical Properties, and Application in Photocatalysis**

*Sabyasachi Maity, André M. T. Muthig, Indranil Sen, Ondřej Mrózek, Andrey Belyaev, Benjamin Hupp, and Andreas Steffen**

Abstract: Cyclic amino(alkyl) and cyclic amino(aryl) carbenes (cAACs/cAArCs) have been established as very useful ligands for catalytic and photonic applications of transition metal complexes. Herein, we describe the synthesis of a structurally related sterically demanding, electrophilic [2.2]isoindolinophanyl-based carbene (iPC) that bears a [2.2]paracyclophane moiety. The latter leads to more delocalized frontier orbitals and intense green fluorescence of (HiPC)OTf (**2**) from an intra-ligand charge transfer (^{1}ILCT) state in the solid state. Base-promoted synthesis of the free carbene led to an unusual ring expansion and subsequent dimerization reaction, but the beneficial ligand properties can be exploited by trapping in situ at a metal center. The iPC ligand is a very potent π-chromophore, which participates in low energy metal-to-ligand (ML)CT transitions in [RhCl(CO)$_2$(iPC)] (**4**) and IL-"through-space"-CT transitions in [Au(iPC)$_2$]OTf (**5**). The steric demand of the iPC leads to high stability of **5** against air, moisture, or solvent attack, and ultralong-lived green phosphorescence with a lifetime of 185 μs is observed in solution. The beneficial photophysical and electronic properties of the iPC ligand, including a large accessible π surface area, were exploited by employing highly efficient energy transfer (EnT) photocatalysis in a [2+2] styrene cycloaddition reaction using **5**, which outperformed other established photocatalysts in comparison.

N-heterocyclic carbenes (NHCs) have become very important spectator ligands in transition metal chemistry to specifically modify the electronic and steric properties of the complexes, which has resulted in a wide range of applications in catalysis and materials science.[1–3] Among the many carbene scaffolds available today, very electrophilic carbenes, such as cyclic amino(alkyl) and cyclic amino(aryl) carbenes (cAAC/cAArC), have been established as potent chromophore ligands in photoactive metal complexes.[4–6] The lowest unoccupied molecular orbital (LUMO) with π-symmetry is suitable to act as an acceptor unit to be involved in low energy metal-to-ligand charge transfer (MLCT) and ligand-to-ligand (LL)CT transitions, providing intense absorption in the visible region of the electromagnetic spectrum. In addition, the metal contribution to the CT mediates strong spin-orbit coupling (SOC), while the significant CT distance can lead to small energy gaps ΔE_{ST} between the singlet and triplet excited states S_1 and T_1, allowing spin-forbidden intersystem-crossing (ISC) $S_1 \rightarrow T_1$ to occur competitively to fluorescence. The triplet excited states in transition metal carbene complexes are often phosphorescent, rendering them interesting candidates for application in OLEDs and other photonic technologies.[2,4,7] Long-lived triplet states are also relevant for photocatalysis via single electron transfer (SET) or energy transfer (EnT), which offers different reaction patterns and product distributions than thermal conversions.[8]

The use of strongly σ-donating, π-electrophilic carbenes as chromophore units has revolutionized the field of photoactive d^{10} metal complexes in particular.[4,5,9,10] Linearly coordinated coinage metal compounds, for example, are now among the most efficient molecular luminophores involving triplet states with exceptional radiative rate constants k_r of up to $4\times10^6\ s^{-1}$ and excellent luminescence quantum yields φ of up to unity.[11–14] However, a potential limitation in the development of useful carbenes for photonic applications is the high reactivity of the ligands themselves as well as of the M–C bond. For instance, while [CuCl(IMes/IDipp)] are stable towards air and moisture,[15] its cAAC and cAArC analogues are highly sensitive,[13,16] requiring careful adjustment of the steric protection. Another challenge for molecular luminophores is the realization of low energy triplet emission in the deep red to near-IR for photonic information technologies,[17] which can be achieved by design of acceptor units with LUMOs of enhanced delocalization resulting in long-distance CT. We found such effects in [Cu(Cz)(carbene)] (Cz = carbazolate) by using the more conjugated cAArC instead of cAAC, leading to an enormous bathochromic emission shift from $\lambda_{max} = 474$ nm to

[*] S. Maity, Dr. A. M. T. Muthig, I. Sen, Dr. O. Mrózek, Dr. A. Belyaev, Dr. B. Hupp, Prof. Dr. A. Steffen
Department of Chemistry and Chemical Biology
TU Dortmund University
Otto-Hahn-Str. 6, 44227 Dortmund, Germany
E-mail: andreas.steffen@tu-dortmund.de

[**] A previous version of this manuscript has been deposited as a preprint on ChemRXiv.

638 nm and 2-fold enhanced k_r of $6.8\times10^5\ s^{-1}$ in polymer matrices.[13] However, the cAArC-based complexes are indeed highly reactive and sensitive towards air and moisture. We are therefore interested in modifying the steric, electronic and photophysical properties of cAArC-like ligands in particular. Inspired by the work of Fürstner and co-workers,[18] who showed for an NHC merged with a paracyclophane (PCP) moiety that some electronic "through-space" communication exists between the two aromatic π-planes, we were curious whether the steric and photophysical properties of cAArC could be beneficially influenced by extension with a PCP unit. Thus, we herein report on the development of an electrophilic [2.2]isoindolinophanyl-based carbene (iPC) that can act as a very potent π-chromophore for photoactive transition metal complexes with potential application in luminescent devices and photocatalysis.

The protonated racemic ligand salt (HiPC)OTf (**2**) could be prepared from 4-bromo-5-formyl[2.2]paracyclophane, which was previously described by Bräse et al.,[19] following the strategy reported for (HcAArC)OTf,[20] except that for the step of imine condensation to obtain **1** we had to add 0.5 eq. $TiCl_4$ as a strong Lewis acid (Figure 1). The product formation of **2** can be observed as a yellow precipitate that fluoresces green under UV irradiation.

The steric and electronic influence of the PCP moiety on the carbene ring system is manifested in the ^{1}H NMR spectrum of the iminium salt **2**, with the resonances of the *ortho* and *meta* hydrogen substituents of the phenyl groups being broad, which suggests limited rotation in solution (Figure S3). Furthermore, the resonances of the methine hydrogens of the Dipp at $\delta = 3.32$ and 0.87 ppm are shifted in comparison to those of cAAC compounds to lower and higher field, respectively, while the methyl groups at $\delta =$ 1.32, 0.72, 0.50 and −0.11 ppm are all found at higher field.

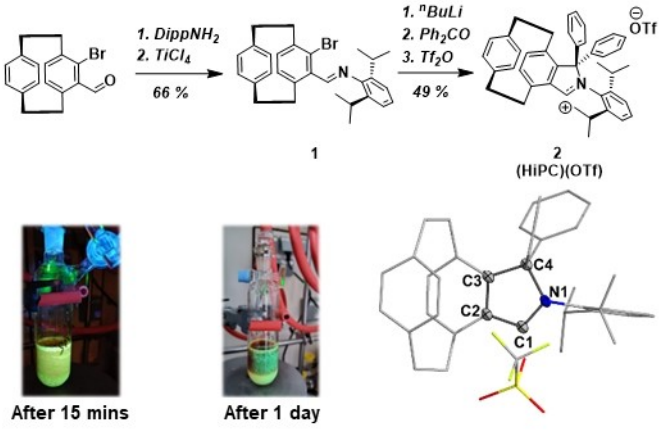

Figure 1. Synthesis and molecular structure of (*S*)-(HiPC)OTf (**2**) determined by SC-XRD studies (hydrogen atoms and (*R*)-isomer omitted for clarity). Photographs show green fluorescence upon UV lamp excitation (360 nm) of **2** precipitating from the reaction mixture. Selected bond lengths (Å) and angles [deg]: C1–C2 1.423(2), C2–C3 1.414(2), C3–C4 1.528(3), C4–N1 1.541(2), N1–C1 1.305(2), C2–C1–N1 112.6(1).

Yellow single crystals of **2** suitable for X-ray diffraction (SC-XRD) studies were obtained from diffusion of diethyl ether into a saturated THF solution. The steric congestion of the PCP fragment leads to an orthogonal arrangement of the phenyl moiety of the "upper hemisphere" with regard to the isoindoline plane, and the Dipp *N*-substituent is bent away from the PCP.

The iminium salt **2** appears yellow in color due to a broad absorption band between 300–475 nm with an extinction coefficient at the maximum of $\varepsilon_{355nm} = 6{,}000\ M^{-1}cm^{-1}$ (Figure 2). According to our TD-DFT calculations, the lowest energy excited states S_1 to S_7 are dominated by CT transitions from the upper aromatic ring of the PCP fragment and the phenyl ring of the same hemisphere to the LUMO, which is delocalized in the bicyclic carbene plane (Figure S51). As noted during the synthesis, **2** shows intense green emission in the solid state with $\lambda_{max} = 520$ nm and a high photoluminescence quantum yield of 0.32, which we assign to fluorescence from the first singlet excited state S_1 according to the short luminescence lifetime of $\tau = 6$ ns. In solution, the emission is broader, and λ_{max} is bathochromically shifted to 585 nm, presumably due to the higher degree of structural reorganization in fluid media and specific solvent interactions of the ^{1}CT state.

Attempts to isolate the free carbene by base-promoted deprotonation, even at low temperatures, were not successful. Instead, the iPC appears to undergo fast C–H insertion of the pendant phenyl ring with subsequent ring expansion, as reported for free cAArCs,[21] and finally C–C coupling of two in-plane PCP moieties would provide dimer **3** (Figure 3, and Figures S8–S11). The mechanism of the last reaction step is not clear, but formal loss of H_2 has occurred as single crystal X-ray diffraction studies suggest C=C double bond formation between the aromatic bridgehead carbon C3 and the ethyl bridge C17. As ^{77}Se NMR of carbene selenium adducts provides useful information on the π-acceptor properties of the free carbene,[22] we thus reacted the iminium salt **2** with a base in the presence of elemental Se, but only dimer **3** could be isolated.

However, the free carbene formed in situ at low temperatures can be trapped by coordination to a metal center as demonstrated by the reaction with $[RhCl(CO)_2]_2$, which led

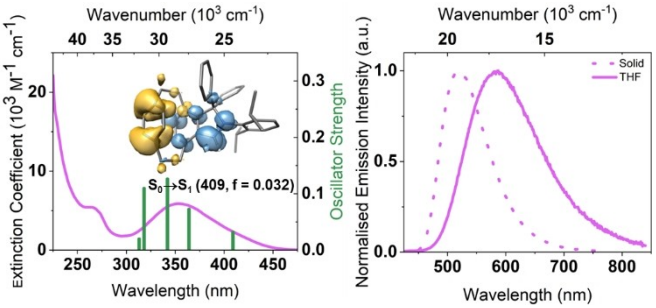

Figure 2. Left: Absorption spectrum of **2** in THF solution, TD-DFT calculated oscillator strengths, and electron density difference of the $S_0 \rightarrow S_1$ transition (loss: yellow, gain: blue). Right: emission spectra of **2** in THF solution (solid) and in the solid state (dotted).

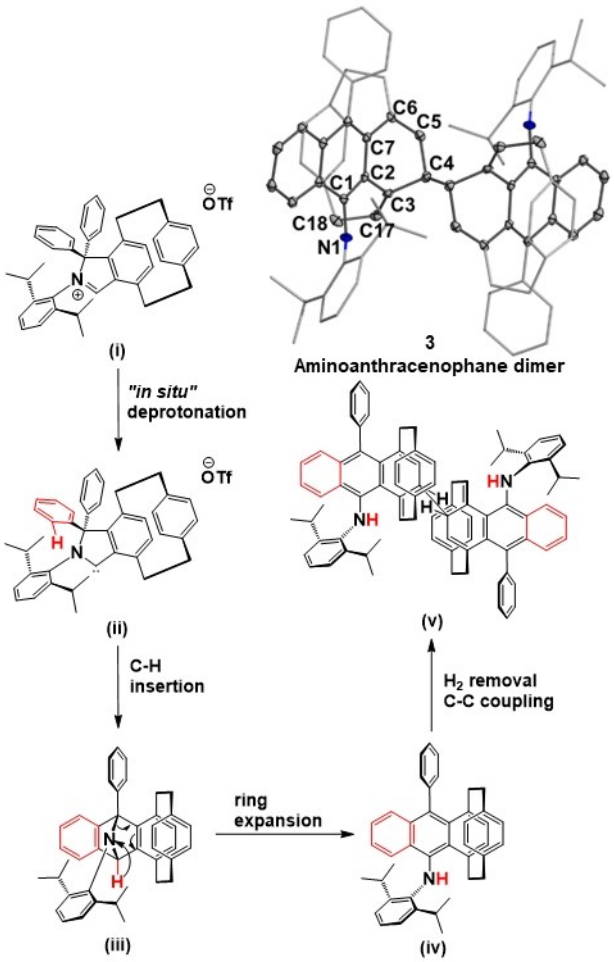

Figure 3. Tentative mechanism for the formation of **3** and its molecular structure determined by SC-XRD. Selected bond lengths (Å) and angles [deg]: C4–C4 1.548(2), C4–C3 1.509(2), C3–C2 1.486(2), C3–C17 1.343(2), C17–C18 1.529(2), C1–N1 1.393(2), C2–C3–C4 112.0(1), C3–C17–C18 126.4(1).

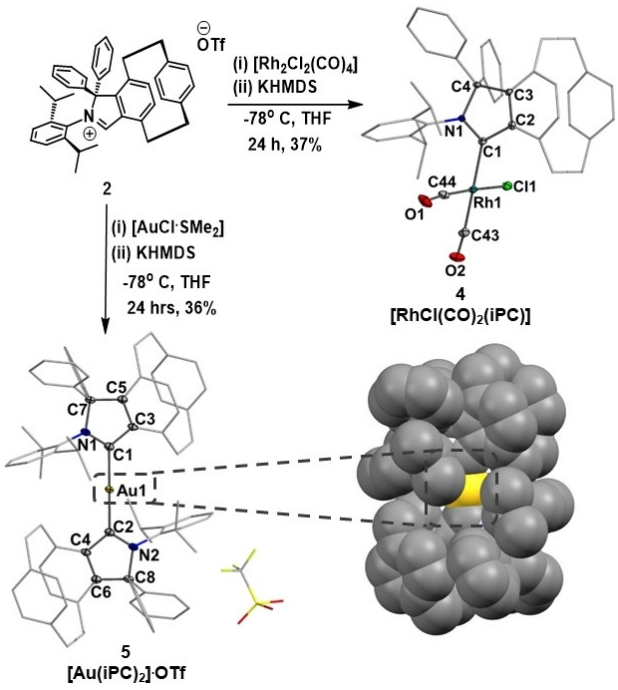

Figure 4. Top: synthesis of Rh^{I} iPC complex **4** and its molecular structure (racemate) determined by SC-XRD. Bottom: synthesis of $[Au(iPC)_2]OTf$ (**5**), its molecular structure (R,S-conformer) determined by SC-XRD studies and space filling model.

to the isolation of racemic square-planar $[RhCl(CO)_2(iPC)]$ (**4**) as confirmed by single crystal X-ray diffraction studies (Figure 4). The ^{13}C NMR resonance of the carbene carbon in **4** is observed at $\delta = 244.6$ ppm as a doublet with $^{1}J_{CRh} = 39$ Hz, while the IR stretching frequencies of the CO ligands are found at 2077 and 1996 cm^{-1}, respectively, giving a Tolman electronic parameter (TEP) of 2050 cm^{-1} (Figures S13 and S35). Thus, the new iPC ligand is a much stronger σ-donor than most NHC ligands and very similar to cAArCs.[23] However, we determined a buried volume V_{bur} of 52 % inflicted by our iPC ligand, while the cAArC covers only 44 % as in [CuCl(cAArC)] (Figures S44 and S45).

The same preparation method as for the Rh^{I} compound **4** can be employed to access the linearly coordinated bis(carbene) gold(I) complex $[Au(iPC)_2]OTf$ (**5**) in good yields (Figure 4), which we isolated as a mixture of the ligand combinations *R,S*, *R,R* and *S,S*. **5** is highly stable even in solution towards air and moisture, although related d^{10} coinage metal cAArC complexes are highly sensitive. The space-filling model obtained from single-crystal X-ray diffraction studies shows that the M–C bonds are sterically protected against nucleophilic attack as the two iPC ligands together occupy 88 % of the volume around the metal center.

Bearing in mind the visible light absorption and fluorescence of the carbene precursor (HiPC)OTf (**2**), and the steric protection that the iPC ligand offers for the metal center, we were curious whether these photophysical properties are maintained upon metal coordination, which is of relevance for future luminescence or photocatalytic applications. Indeed, the rhodium(I) complex **4** exhibits broad absorption bands in the visible between 350–520 nm with extinction coefficients of ca. $\varepsilon = 2{,}500$–$4{,}500\ M^{-1}cm^{-1}$ at the respective maxima due to CT transitions that often involve the iPC ligand (Figure 5). The lowest energy vertical singlet transition $S_0 \rightarrow S_1$ is dominated by a $Rh(d_z^2) \rightarrow iPC(\pi^*)$ CT, which is responsible for the orange color of **4**. This band is bathochromically shifted due to the more delocalized LUMO of the iPC ligand and the resulting longer CT distance in comparison to other $[RhCl(NHC)(CO)_2]$ complexes or the cAArC analogue, which have been described as yellow powders. The S_2 state originates from an iPC ^{1}ILCT and the S_3 state is $Rh(d_z^2) \rightarrow CO(\pi^*)$ CT in nature (Figure S52). The energetically higher lying singlet transitions are complex mixtures of those already described and exhibit significantly higher oscillator strengths, thus explaining the higher ε values in the UV region.

Upon UV irradiation of **4** in solution at 365 nm, blue fluorescence with $\lambda_{max} = 450$ nm from a high energy ^{1}ILCT state of the iPC ligand is observed, indicating that internal

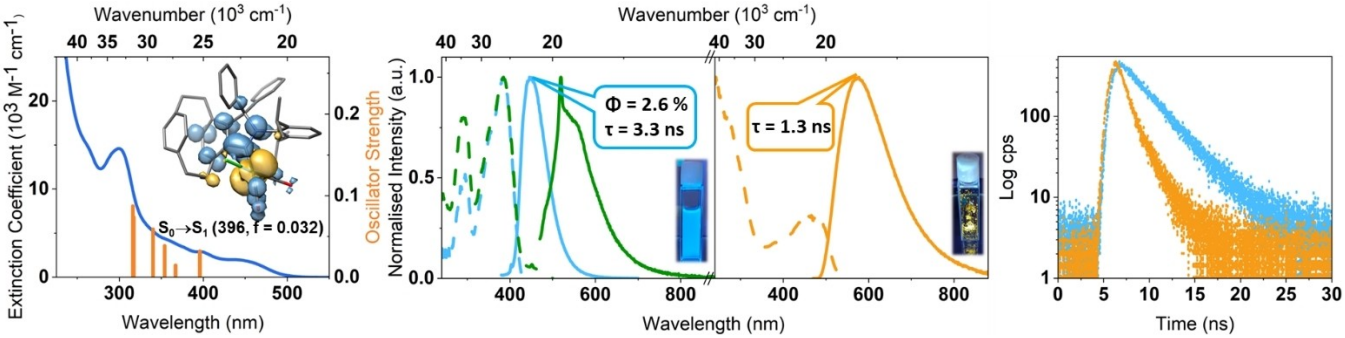

Figure 5. Left to right: Absorption spectrum of **4** in THF, TD-DFT calculated oscillator strengths, and electron density difference of the $S_0 \rightarrow S_1$ transition (loss: yellow, gain: blue), fluorescence (solid) spectra in THF solution (sky blue: $\lambda_{ex} = 360$ nm, green: $\lambda_{ex} = 450$ nm, the sharp spike at 520 nm is due to scattering), fluorescence (solid) in the solid state (orange; $\lambda_{ex} = 450$ nm), and respective excitation spectra (dashed), fluorescence lifetime decays in THF solution (sky blue, $\lambda_{em} = 450$ nm) and in the solid state (orange, $\lambda_{em} = 575$ nm).

conversion (IC) to the S_1 state and ISC are both slow (Figure 5). However, excitation in the lowest energy absorption band at 450 nm gives weak yellow fluorescence from the ^{1}MLCT state with a short lifetime of 1.3 ns in the solid state due to inefficient SOC from Rh and slow ISC $S_1 \rightarrow T_1$, with no phosphorescence observable even at 77 K in 2-MeTHF or in the solid state (Figures S39–43), similar to 2,5-aryl-ethynylrhodacyclopenta-2,5-dienes reported by Marder et al.[23]

The absorption spectrum of the gold(I) bis(iPC) complex **5** is similar to that of (HiPC)OTf (**2**), with broad low energy absorption bands that reach out into the visible region of the electromagnetic spectrum to 425 nm, albeit with smaller extinction coefficients ($\varepsilon_{350nm} = 1{,}850\ M^{-1}cm^{-1}$) (Figure 6). According to our TD-DFT calculations, the latter finding is due to the photophysical ground state properties of **5** being dominated by ^{1}IL "through-space" CT transitions with

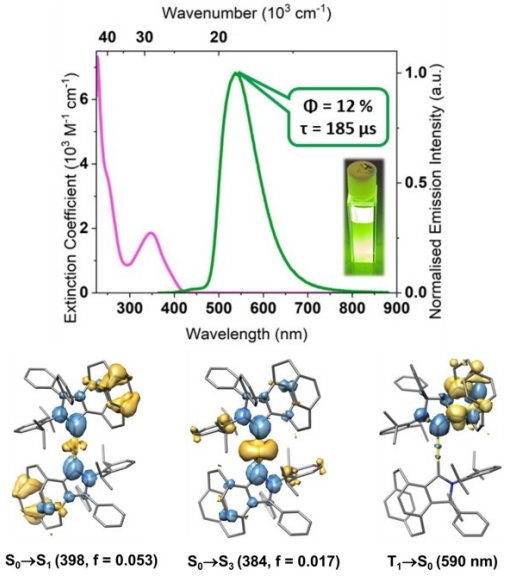

Figure 6. Top: absorption (purple) and emission (green) spectra of [Au(iPC)$_2$]OTf (**5**) in CH_2Cl_2 solution. Bottom: TD-DFT electron density differences of selected transitions of S,R-**5** (loss: yellow, gain: blue).

MLCT admixtures, except for the $S_0 \rightarrow S_3$ transition, which is Au(d_z^2)→iPC(π^*) in nature. We note that the calculated absorption properties of the different diastereomers of **5** are very similar and cannot be experimentally distinguished from each other due to the broad spectral character (see also Figures S53–54, and Tables S13–14).

While **2** undergoes efficient spin-allowed fluorescence on the nanosecond timescale only in the solid state due to facile non-radiative decay in solution, the enhanced rigidity imposed by the iPC ligands and SOC mediated by the Au^I ion in **5** leads to ultralong-lived green phosphorescence ($\lambda_{max} = 540$ nm) with $\tau = 185$ µs and $\varphi = 0.12$ in CH_2Cl_2 solution from a ^{3}ILCT state, of which the assignment is supported by DFT calculations (Figure 6, and Figure S54). The broad spectral appearance and its excited state lifetime combined with the large accessible surface area of the iPC ligands render [Au(iPC)$_2$]OTf (**5**) a potentially useful photocatalyst by energy transfer (EnT). Indeed, its application in 1 mol-% catalyst loading for the [2+2] cycloaddition of (E,E′)-dicinnamyl ether led to full conversion to the desired product upon irradiation at 405 nm for 2 hours (Scheme 1). ^{1}H NMR spectroscopic studies and UV/Vis absorption measurements upon exposure of complex **5** in the presence of 1 eq. of the organic substrate to 405 nm light irradiation shows that the photocatalyst is stable under the reaction conditions (Figures S46–47). Also, the photoinduced reaction occurs without induction period, which excludes formation of a photocatalytically active impurity being responsible for the product formation.

The EnT of **5** to the substrate appears to be much more efficient in comparison to many other well-established photocatalysts[24] that have been tested in this application scenario because the required reaction time is significantly shorter, although we have excited at the low energy absorption edge with small $\varepsilon_{405} = 300\ M^{-1}cm^{-1}$.

We have developed a new electrophilic [2.2]isoindolinophanyl-based carbene, which is structurally related to previously reported cAAC and cAArC ligands, with very similar σ-donor strength. However, the para-cyclophane moiety is electronically coupled to the carbene framework and facilitates visible light absorption and ^{1}ILCT

[2+2] Cycloaddition of (E,E')-Dicinnamyl Ether

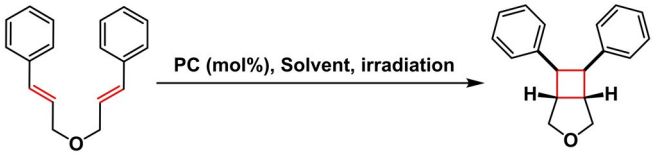

Photocatalysts (loading)	λ_{ex}	Solvent	Time	Yield
$[Ir(dF(CF_3)ppy)_2(dtbbpy)]PF_6$ (1 mol%)	CFL	DMSO	4 h	89 %
[Au(Cz)(SIPr)] (5 mol%)	365 nm	THF	4 h	>99 %
[Pd-B-1] (1 mol%)	>350 nm	ACN	3 h	88 %
[Pd-N-1] (1 mol%)	462 nm	ACN	4 h	97 %
$[Au(iPC)_2]OTf$ (**5**) (1 mol%)	405 nm	DCM	2 h	>99 %

Scheme 1. [2+2] cycloaddition of (E,E')-dicinnamyl ether by photo-induced EnT using **5** as a catalyst, and comparison with other established photocatalysts ($dF(CF_3)ppy$ = 2-(2,4-difluorophenyl)-5-trifluoromethylpyridine, dtbbpy = 4,4′-di-tert-butyl-2,2′-dipyridyl, SIPr = 1,3-bis(2,6-diisopropylphenyl)-2-imidazolidinylidene, Pd–B-1 and Pd–N-1 = see Figure S55). CFL = candescent fluorescence lamp.

fluorescence of the salt (HiPC)OTf (**2**). The beneficial photophysical properties of the iPC can be transferred to its metal complexes $[RhCl(CO)_2(iPC)]$ (**4**) and $[Au(iPC)_2]OTf$ (**5**), where it acts as a very potent excited state π-acceptor ligand and yellow ^{1}MLCT fluorescence and ^{3}ILCT/MLCT "through space" phosphorescence are observed, respectively. The large steric demand of the iPC ligand in homoleptic **5** leads to a very long lifetime of 185 µs of the excited state with a quantum yield of 12 % in solution, and in combination with the extended π-surface highly efficient triplet EnT for photocatalytic applications can be realized.

Supporting Information

The authors have cited additional references within the Supporting Information.[26–38]

Acknowledgements

We thank MSc. Paul Ruer for assistance with the collection of some of the SC-XRD data. This work was supported by Deutsche Forschungsgemeinschaft [DFG, Priority Program SPP 1928 "COORNETs—Koordinationsnetzwerke als Bausteine für Funktionssysteme" (STE1834/9-1)]. Open Access funding enabled and organized by Projekt DEAL.

Conflict of Interest

The authors declare no conflict of interest.

Data Availability Statement

The data that support the findings of this study are available in the supplementary material of this article.

Keywords: Carbene · Paracyclophane · Luminescence · Coordination Chemistry · Photocatalysis

[1] a) F. E. Hahn, *Chem. Rev.* **2018**, *118*, 9455; b) M. N. Hopkinson, C. Richter, M. Schedler, F. Glorius, *Nature* **2014**, *510*, 485.
[2] H. Amouri, *Chem. Rev.* **2023**, *123*, 230.
[3] a) R. Jazzar, M. Soleilhavoup, G. Bertrand, *Chem. Rev.* **2020**, *120*, 4141; b) B. Hupp, J. Nitsch, T. Schmitt, R. Bertermann, K. Edkins, F. Hirsch, I. Fischer, M. Auth, A. Sperlich, A. Steffen, *Angew. Chem. Int. Ed.* **2018**, *57*, 13671; c) L. Zapf, S. Peters, U. Radius, M. Finze, *Angew. Chem. Int. Ed.* **2023**, *62*, e202300056.
[4] A. Steffen, B. Hupp, in *Comprehensive Coordination Chemistry III* (Eds.: E. C. Constable, G. Parkin, L. Que Jr), Elsevier, Oxford **2021**, pp. 466.
[5] T.-Y. Li, S.-J. Zheng, P. I. Djurovich, M. E. Thompson, *Chem. Rev.* **2024**, *124*, 4332.
[6] a) S. Bai, Y.-F. Han, *Acc. Chem. Res.* **2023**, *56*, 1213; b) C. M. Hendrich, K. Sekine, T. Koshikawa, K. Tanaka, A. S. K. Hashmi, *Chem. Rev.* **2021**, *121*, 9113; c) J. Beaudelot, S. Oger, S. Peruško, T.-A. Phan, T. Teunens, C. Moucheron, G. Evano, *Chem. Rev.* **2022**, *122*, 16365.
[7] a) F. Wurl, S. Stipurin, J. I. Kollar, T. Strassner, *Angew. Chem. Int. Ed.* **2023**, *62*, e202301225; b) A. K. Pal, S. Krotkus, M. Fontani, C. F. R. Mackenzie, D. B. Cordes, A. M. Z. Slawin, I. D. W. Samuel, E. Zysman-Colman, *Adv. Mater.* **2018**, *30*, 1804231.
[8] a) M. A. Bryden, F. Millward, O. S. Lee, L. Cork, M. C. Gather, A. Steffen, E. Zysman-Colman, *Chem. Sci.* **2024**, *15*, 3741; b) J. Twilton, C. Le, P. Zhang, M. H. Shaw, R. W. Evans, D. W. C. MacMillan, *Nat. Chem. Rev.* **2017**, *1*, 0052; c) S. Dutta, J. E. Erchinger, F. Strieth-Kalthoff, R. Kleinmans, F. Glorius, *Chem. Soc. Rev.* **2024**, *53*, 1068.
[9] a) D. Di, A. S. Romanov, L. Yang, J. M. Richter, J. P. H. Rivett, S. Jones, T. H. Thomas, M. Abdi Jalebi, R. H. Friend, M. Linnolahti, M. Bochmann, *Science* **2017**, *356*, 159; b) R. Hamze, J. L. Peltier, D. Sylvinson, M. Jung, J. Cardenas, R. Haiges, M. Soleilhavoup, R. Jazzar, P. I. Djurovich, G. Bertrand M E Thompson, *Science* **2019**, *363*, 601.
[10] a) M. Mitra, O. Mrózek, M. Putscher, J. Guhl, B. Hupp, A. Belyaev, C. M. Marian, A. Steffen, *Angew. Chem. Int. Ed.* **2024**, *63*, e202316300; b) O. Mrózek, M. Mitra, B. Hupp, A. Belyaev, N. Lüdtke, D. Wagner, C. Wang, O. S. Wenger, C. M. Marian, A. Steffen, *Chem. Eur. J.* **2023**, *29*, e202203980.
[11] C. N. Muniz, J. Schaab, A. Razgoniaev, P. I. Djurovich, M. E. Thompson, *J. Am. Chem. Soc.* **2022**, *144*, 17916.
[12] T.-Y. Li, S.-J. Zheng, P. I. Djurovich, M. E. Thompson, *Chem. Rev.* **2024**, *124*, 4332.
[13] M. Gernert, L. Balles-Wolf, F. Kerner, U. Müller, A. Schmiedel, M. Holzapfel, C. M. Marian, J. Pflaum, C. Lambert, A. Steffen, *J. Am. Chem. Soc.* **2020**, *142*, 8897.
[14] A. Ruduss, A. Jece, K. A. Stucere, K.-W. Chen, B. Turovska, S. Belyakov, A. Vembris, C.-H. Chang, K. Traskovskis, *J. Mater. Chem. C* **2024**, *12*, 2968.
[15] H. G. Raubenheimer, S. Cronje, P. J. Olivier, *J. Chem. Soc. Dalton Trans.* **1995**, 313.
[16] M. Gernert, U. Müller, M. Haehnel, J. Pflaum, A. Steffen, *Chem. Eur. J.* **2017**, *23*, 2206.
[17] a) H. Xiang, J. Cheng, X. Ma, X. Zhou, J. J. Chruma, *Chem. Soc. Rev.* **2013**, *42*, 6128; b) Y. Zheng, X. Zhu, *Org. Mat.* **2020**, *02*, 253; c) M. Vasilopoulou, A. Fakharuddin, F. P. Gar-

cía de Arquer, D. G. Georgiadou, H. Kim, A. R. b Mohd Yusoff, F. Gao, M. K. Nazeeruddin, H. J. Bolink, E. H. Sargent, *Nat. Photonics* **2021**, *15*, 656; d) M. Nothaft, S. Höhla, F. Jelezko, N. Frühauf, J. Pflaum, J. Wrachtrup, *Nat. Commun.* **2012**, *3*, 628.
[18] a) A. Fürstner, M. Alcarazo, H. Krause, C. W. Lehmann, *J. Am. Chem. Soc.* **2007**, *129*, 12676; b) M. Alcarazo, T. Stork, A. Anoop, W. Thiel, A. Fürstner, *Angew. Chem. Int. Ed.* **2010**, *49*, 2542.
[19] J. J. P. Kramer, C. Yildiz, M. Nieger, S. Bräse, *Eur. J. Org. Chem.* **2014**, *2014*, 1287.
[20] B. Rao, H. Tang, X. Zeng, L. L. Liu, M. Melaimi, G. Bertrand, *Angew. Chem. Int. Ed.* **2015**, *54*, 14915.
[21] J. Lorkowski, M. Krahfuß, M. Kubicki, U. Radius, C. Pietraszuk, *Chem. Eur. J.* **2019**, *25*, 11365.
[22] T. Hölzel, C. Ganter, *J. Organomet. Chem.* **2020**, *915*, 121234.
[23] a) C. Sieck, M. G. Tay, M.-H. Thibault, R. M. Edkins, K. Costuas, J.-F. Halet, A. S. Batsanov, M. Haehnel, K. Edkins, A. Lorbach, A. Steffen, T. B. Marder, *Chem. Eur. J.* **2016**, *22*, 10523; b) A. Steffen, M. G. Tay, A. S. Batsanov, J. A. K. Howard, A. Beeby, K. Q. Vuong, X.-Z. Sun, M. W. George, T. B. Marder, *Angew. Chem. Int. Ed.* **2010**, *122*, 2399.
[24] a) P.-K. Chow, G. Cheng, G. S. M. Tong, C. Ma, W.-M. Kwok, W.-H. Ang, C. Y.-S. Chung, C. Yang, F. Wang, C.-M. Che, *Chem. Sci.* **2016**, *7*, 6083; b) Z. Lu, T. P. Yoon, *Angew. Chem. Int. Ed.* **2012**, *51*, 10329; c) N. V. Tzouras, E. A. Martynova, X. Ma, T. Scattolin, B. Hupp, H. Busen, M. Saab, Z. Zhang, L. Falivene, G. Pisanò, et al., *Chem. Eur. J.* **2021**, *27*, 11904.
[25] Deposition numbers 2271625 (for **2**), 2271626 (for **3**), 2271627 (for **4**), and 2349442 (for **5**) contain the supplementary crystallographic data for this paper. These data are provided free of charge by the joint Cambridge Crystallographic Data Centre and Fachinformationszentrum Karlsruhe Access Structures service.
[26] W. L. F. Armarego, *Purification of laboratory Chemicals*, Butterworth Heinemann, Oxford; Boston **1996**.
[27] G. M. Sheldrick, *Acta Crystallogr. Sect. C* **2015**, *71*, 3.
[28] O. V. Dolomanov, L. J. Bourhis, R. J. Gildea, J. A. K. Howard, H. Puschmann, *J. Appl. Crystallogr.* **2009**, *42*, 339.
[29] A. L. Spek, *Acta Crystallogr.* **2015**, *71*, 9.
[30] a) L. Falivene, Z. Cao, A. Petta, L. Serra, A. Poater, R. Oliva, V. Scarano, L. Cavallo, *Nat. Chem.* **2019**, *11*, 872 ; b) A. Poater, F. Ragone, S. Giudice, C. Costabile, R. Dorta, S. P. Nolan, L. Cavallo, *Organometallics* **2008**, *27*, 2679; c) A. Poater, F. Ragone, R. Mariz, R. Dorta, L. Cavallo, *Chem. Eur. J.* **2010**, *16*, 14348.
[31] F. Neese, *WIREs Comput. Mol. Sci.* **2012**, *2*, 73.
[32] a) C. Adamo, V. Barone, *J. Chem. Phys.* **1999**, *110*, 6158; b) J. P. Perdew, K. Burke, M. Ernzerhof, *Phys. Rev. Lett.* **1996**, *77*, 3865; c) J. P. Perdew, K. Burke, M. Ernzerhof, *Phys. Rev. Lett.* **1997**, *78*, 1396; d) C. Cardoso, A. T. Costa, A. H. MacDonald, J. Fernández-Rossier, *Phys. Rev. B Condens. Matter.* **1996**, *105*, 9982; e) M. Ernzerhof, G. E. Scuseria, *J. Chem. Phys.* **1999**, *110*, 5029; f) J. Tao, J. P. Perdew, V. N. Staroverov, G. E. Scuseria, *Phys. Rev. Lett.* **2003**, *91*, 146401; g) J. P. Perdew, J. Tao, V. N. Staroverov, G. E. Scuseria, *J. Chem. Phys.* **2004**, *120*, 6898.
[33] a) A. Schäfer, H. Horn, R. Ahlrichs, *J. Chem. Phys.* **1992**, *97*, 2571; b) F. Weigend, R. Ahlrichs, *Phys. Chem. Chem. Phys.* **2005**, *7*, 3297.
[34] a) S. Grimme, J. Antony, S. Ehrlich, H. Krieg, *J. Chem. Phys.* **2010**, *132*, 154104; b) S. Grimme, S. Ehrlich, L. Goerigk, *J. Comput. Chem.* **2011**, *32*, 1456.
[35] a) F. Weigend, *Phys. Chem. Chem. Phys.* **2006**, *8*, 1057; b) D. A. Pantazis, F. Neese, *J. Chem. Theory Comput.* **2009**, *5*, 2229; c) D. A. Pantazis, F. Neese, *Theor. Chem. Acc.* **2012**, *131*, 1292; d) D. A. Pantazis, F. Neese, *J. Chem. Theory Comput.* **2011**, *7*, 677.
[36] V. Barone, M. Cossi, *J. Phys. Chem. A* **1998**, *102*, 1995.
[37] D. A. Pantazis, X. Y. Chen, C. R. Landis, F. Neese, *J. Chem. Theory Comput.* **2008**, *4*, 908.
[38] E. F. Pettersen, T. D. Goddard, C. C. Huang, G. S. Couch, D. M. Greenblatt, E. C. Meng, T. E. Ferrin, *J. Comput. Chem.* **2004**, *13*, 1605.

Manuscript received: May 14, 2024
Accepted manuscript online: July 4, 2024
Version of record online: September 5, 2024